Free Vibration Analysis of a Rectangular Duct with Different Axial Boundary Conditions

Pruthviraj Namdeo Chavan and B. Venkatesham

Department of Mechanical Engineering, Indian Institute of Technology Hyderabad, Ordnance Factory Estate, Yeddumailaram, 502205, A.P., India.

(Received 18 August 2012; revised 27 March 2014; accepted 7 May 2014)

This paper describes the free vibration analysis of a rectangular duct by using the Rayleigh-Ritz method. Static beam functions are used as admissible functions in the Rayleigh-Ritz method. These basis functions are the static solutions of a point-supported beam under a series of sinusoidal loads. The unique advantage of using this method is that it allows for the consideration of different axial boundary conditions of a duct. Computational results are validated with existing literature data for a simply supported rectangular duct and the finite element method (FEM) for other axial boundary conditions. A validated analytical model is used for generating natural frequency data for different dimensions of rectangular ducts. Further curve fitting has been done for the generated data, and an empirical relation has been presented to calculate the first fundamental natural frequency for different material properties of ducts and different axial boundary conditions, which can be used for any dimensions of the duct within the specified range.

1. INTRODUCTION

Heating, Ventilation, and Air Conditioning (HVAC) systems extensively use ducts of different sizes and shapes that are connected in series or in parallel for air-handling purposes. The most prominent duct shapes are circular, rectangular, and elliptical. Noise generated from air handling units propagates in the axial and transverse directions of a duct. Noise radiated from ducts in the transverse direction is called breakout noise. Rectangular ducts have the highest breakout noise compared to a circular duct's cross-section due to lower stiffness. The breakout noise from these ducts has an impact at lower frequencies. The coupling of acoustic duct modes and structural duct modes plays a critical role in generating noise in the transverse direction. The first step in understanding structural-acoustic coupling is to calculate the natural frequencies and mode shapes of the structural components. The research interest in this paper is the free vibration analysis of rectangular ducts.

Different methods have been proposed in literature for free vibration analysis of polygonal ducts. S. Azimi et al. and G. Yamada et al. used the receptance method.[1,2] H. P. Lee used the Rayleigh-Ritz method for calculating the natural frequencies and the mode shape of cylindrical polygonal ducts, in which sinusoidal functions are used as admissible functions.[3] T. Irea, et al. used the transfer matrix method for free vibration analysis of prismatic shells.[4] Sai Jagan Mohan et al. used the Finite Element Method (FEM) to calculate the duct natural frequencies and the mode shape.[5] They used group theoretical analysis to characterize duct modes. Existing literature results have only considered simply supported boundary conditions in the axial direction of the duct. According to current research, there is no work reported for the other axial boundary conditions. So in the present paper, the Rayleigh-Ritz method, which is capable of considering different axial boundary conditions, is used for calculating the natural frequencies of rectangular ducts.

A good amount of literature is available for the Rayleigh-Ritz methods with different admissible functions. Selection of proper admissible functions provides variation in the Rayleigh-Ritz method. Admissible function varies based on applications like rectangular plates, rectangular plates with intermediate supports, etc. Zhou Ding used the Rayleigh-Ritz method for natural frequency analysis of rectangular plates with a set of static beam functions as admissible functions.[6] D. Zhou et al. used a set of static beam functions for free vibration analysis of rectangular plates with intermediate supports.[7] In the present paper, rectangular ducts are modelled as unfolded plates with rotational springs, and the creases are modelled as intermediate supports. The set of static beam functions are extended for the rectangular ducts. In the Rayleigh-Ritz method, validity and accuracy are entirely dependent on the choice of the admissible functions.[8] These static beam functions are the static solutions of the point-supported beams under sinusoidal loads.

Calculated results from this method are validated with the data from the literature and with the FEM results. The validated analytical model is used to generate the engineering data for the rectangular ducts with different side ratios (height to width or width to height of the duct) and with different aspect ratios (perimeter of the duct cross section to length of the duct). These ratios are taken as four-step values (0.25, 0.5, 0.75, and 1). Further curve fitting has been done for generated engineering data results, and an empirical relation has been developed to calculate the first fundamental frequency. This empirical relation can be used to calculate the first fundamental frequency for any combination of an aspect ratio and a side ratio between a range of 0.25 to 1 with a prediction accuracy of 95%.

Figure 1 shows the rectangular duct with dimensions of L_1, L_2, and L_3 in X, Y, and Z directions, respectively. The reference coordinate system is also shown in Fig. 1.

2. THE RAYLEIGH-RITZ METHOD

The main advantage of this present Rayleigh-Ritz method with the static beam function as an admissible function is that

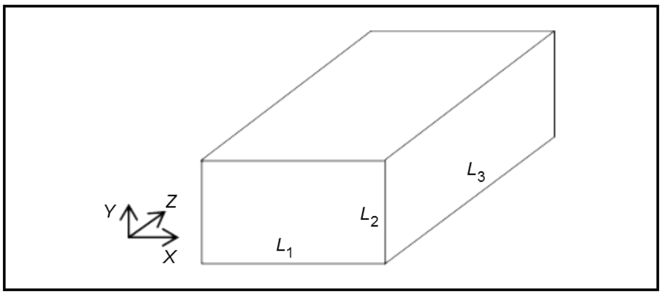

Figure 1. A schematic diagram of a rectangular duct.

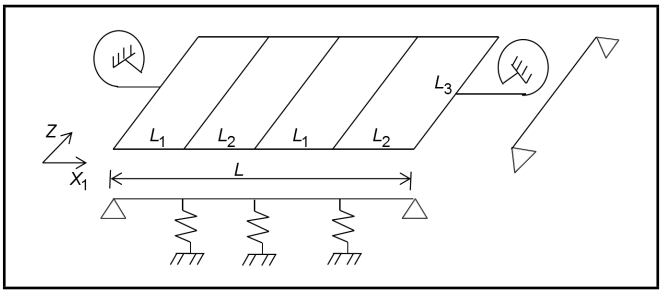

Figure 2. An unfolded plate representation of a simply supported rectangular duct.

it has the capability to choose boundary conditions in the axial direction. The different axial boundary conditions considered are Simple-Simple (S-S), Clamped-Clamped (C-C), Clamped-Simple (C-S), and Clamped-Free (C-F).

Figure 2 shows the unfolded representation of the rectangular duct shown in Fig. 1. It consists of four flat plates connected side-by-side with intermediate supports that are represented, and the ends with torsional springs as shown in Fig. 2. Thus, it can be approximated as a beam with three intermediate supports in the X_1-direction and a simple supported beam in the axial direction (Z-direction).

2.1. The Rayleigh-Ritz Approach

For the free vibration analysis of plate, the deflection w can be expressed as

$$w(x, y, t) = W(x, y)e^{i\omega t}; \tag{1}$$

where ω is the eigenfrequency of plate vibration, t is the time, and $i = \sqrt{-1}$. Assuming,

$$\xi = x/L; \qquad \eta = z/L^3. \tag{2}$$

The mod shape function $W(\xi, \eta)$ can be expressed in terms of the series function as follows,

$$W(\xi, \eta) = \sum_{m=1}^{\infty}\sum_{n=1}^{\infty} A_{mn}\phi_m(\xi)\psi_n(\eta); \tag{3}$$

where $\phi_m(\xi)$ and $\psi_n(\eta)$ are the admissible functions in the circumferential and axial directions, respectively. A_{mn} are unknown coefficients. By minimizing the total energy for thin plates as follows

$$\frac{\partial}{\partial A_{mn}}\left(U_{\max} - T_{\max}\right) = 0; \tag{4}$$

$U_{\max}$ and $T_{\max}$ are maximum potential and kinetic energies for the thin plates obtained by using the vibration theory of thin plates. Equation (4) leads to the eigenfrequency equation, which is given as

$$\sum_{m=1}^{\infty}\sum_{n=1}^{\infty}\left[C_{mnij} - \lambda^2 E_{mi}^{(0,0)} F_{nj}^{(0,0)}\right] A_{mn} = 0; \tag{5}$$

where

$$\begin{aligned} C_{mnij} = {} & E_{mi}^{(2,2)} F_{nj}^{(0,0)} + E_{mi}^{(0,0)} F_{nj}^{(2,2)}/\gamma^4 + \\ & \nu\left(E_{mi}^{(0,2)} F_{nj}^{(2,0)} + E_{mi}^{(2,0)} F_{nj}^{(0,2)}/\gamma^2\right) + \\ & 2(1-\nu)\left(E_{mi}^{(1,1)} F_{nj}^{(1,1)}/\gamma^2\right); \\ \lambda^2 = {} & \rho h \omega^2 L_3^4/H; \\ \gamma = {} & L/L_3; \\ E_{mi}^{(r,s)} = {} & \int_0^1 \left(d^r\phi_m/d\xi^r\right)\left(d^s\phi_i/d\xi^s\right) d\xi; \\ F_{nj}^{(r,s)} = {} & \int_0^1 \left(d^r\psi_n/d\eta^r\right)\left(d^s\psi_j/d\eta^s\right) d\eta; \end{aligned} \tag{6}$$

$\rho =$ density, $h =$ thickness, $L =$ perimeter of rectangular duct, and $H = Eh^3/(12 * (1 - \nu^2))$.

As discussed, the validity and accuracy of the Rayleigh-Ritz method entirely depends upon the choice of the admissible function. The appropriate admissible function should at least satisfy the geometrical boundary conditions and, if possible, all the boundary conditions. In the presented method, these admissible functions are taken as a set of static beam functions. So,

$$\begin{aligned} \phi_m(\xi) &= y_m(\xi); \\ \psi_n(\eta) &= y_n(\eta); \end{aligned} \tag{7}$$

$y_m(\xi)$ and $y_n(\eta)$ are the m^{th} and n^{th} static beam functions in the X_1 and Z directions, respectively. These functions satisfy the geometrical boundary conditions and the zero deflection condition at the line supports.

2.2. Static Beam Functions

The static beam functions for the rectangular plate with three intermediate supports in X_1-direction are given in the references.[7] The static beam function in the axial direction can be considered as the deflection of a beam with end supports.[6] The deflection $y(\xi)$ of the beam in the circumferential direction can be written as

$$y_m(\xi) = \sum_{k=0}^{3} C_k^m \xi^k + \sum_{j=1}^{3} P_j^m \frac{(\xi - \xi_j)^3}{6} U(\xi - \xi_j) + \sin(m\pi\xi). \tag{8}$$

The deflection $y(\eta)$ of the beam in the axial direction can be written as

$$y_n(\eta) = \sum_{k=0}^{3} C_k^n \eta^k + \sin(n\pi\eta); \tag{9}$$

where P_j^m $(j = 1, 2, 3)$ and C_k^m $(k = 0, 1, 2, 3)$ are unknown coefficients, and $U(\xi - \xi_j)$ is a Heaviside function.

By observing Eqs. (8) and (9), the second series term is missing in Eq. (9) because the plate has intermediate supports in the circumferential direction and also continues in the axial direction.

The unknowns in Eqs. (8) and (9) can be uniquely decided by using the boundary conditions and zero deflection conditions at the intermediate supports. This can be written in the matrix form as $W(\xi,\eta) = \sum_{m=1}^{\infty}\sum_{n=1}^{\infty} A_{mn}\phi_m(\xi)\psi_n(\eta)$.

$$\begin{bmatrix}\mathbf{A} & \mathbf{D}\\ \mathbf{T} & \mathbf{G}\end{bmatrix}\begin{bmatrix}\mathbf{C}^m\\ \mathbf{P}^m\end{bmatrix} = \begin{bmatrix}\mathbf{R}^m\\ \mathbf{S}^m\end{bmatrix}; \tag{10}$$

where $\mathbf{A}$ is $J \times 4$ matrix, $\mathbf{T}$ is 4×4 matrix, and they refer to the first series terms of equations. $\mathbf{D}$ is $J \times J$ matrix, $\mathbf{G}$ is $4 \times J$ matrix, and they refer to the second series terms of the equation. $\mathbf{R}^m$ is $J \times 1$ matrix, $\mathbf{S}^n$ is 4×1 matrix, and they refer to the third term of the equation for the boundary conditions of the beam. $\mathbf{C}^m$ and $\mathbf{P}^m$ are unknown coefficient matrices as follows:

$$\mathbf{C}^m = \begin{bmatrix}C_0^m & C_1^m & C_2^m & C_3^m\end{bmatrix}^T;$$
$$\mathbf{P}^m = \begin{bmatrix}P_1^m & P_2^m & P_3^m\end{bmatrix}^T. \tag{11}$$

Generally $\mathbf{A}$, $\mathbf{D}$ and $\mathbf{R}^i$ matrices are given as

$$\mathbf{A} = \begin{bmatrix}1 & \xi_1 & \xi_1^2 & \xi_1^3\\ 1 & \xi_2 & \xi_2^2 & \xi_2^3\\ \vdots & \vdots & \vdots & \vdots\\ 1 & \xi_J & \xi_J^2 & \xi_J^3\end{bmatrix};$$

$$\mathbf{R}^m = \begin{bmatrix}-\sin(m\pi\xi_1)\\ -\sin(m\pi\xi_2)\\ \vdots\\ -\sin(m\pi\xi_J)\end{bmatrix};$$

$$\mathbf{D} = \begin{bmatrix}0 & 0 & 0 & \cdots & 0\\ \frac{(\xi_2-\xi_1)^3}{6} & 0 & 0 & \cdots & 0\\ \frac{(\xi_3-\xi_1)^3}{6} & \frac{(\xi_3-\xi_2)^3}{6} & 0 & \cdots & 0\\ \vdots & \vdots & \vdots & \vdots & \vdots\\ \frac{(\xi_J-\xi_1)^3}{6} & \frac{(\xi_J-\xi_2)^3}{6} & \cdots & \frac{(\xi_J-\xi_{J-1})^3}{6} & 0\end{bmatrix}; \tag{12}$$

where J is the number of intermediate supports that are three in the circumferential direction and zero in the axial direction. So in the axial direction the matrices $\mathbf{A}$, $\mathbf{D}$, $\mathbf{G}$, $\mathbf{R}^m$, and $\mathbf{P}^m$ will be zero.

Clamped, simply supported, and free-boundary conditions are denoted by C, S, and F. The elements of the matrices $\mathbf{T}$, $\mathbf{G}$, and $\mathbf{S}_i$ according to the boundary conditions of the beam are

- $T_{11} = T_{22} = 1$, $S_2^n = -n\pi$ for the beam with C as the left end;
- $T_{11} = 1, T_{23} = 2$ for the beam with S as the left end;
- $T_{13} = 2$, $T_{24} = 6$, $S_2^n = (n\pi)^2$ for the beam with F as the left end;
- $T_{31} = T_{32} = T_{33} = T_{34} = 1$, $T_{42} = 1$, $T_{43} = 3$, $G_{3j} = (1-\xi_j)^3/6$, $G_{4j} = (1-\xi_j)^2/2$, $S_4^n = -n\pi(-1)^n$ for the beam with C as the right end;
- $T_{31} = T_{32} = T_{33} = T_{34} = 1$, $T_{43} = 2$, $T_{44} = 6$, $G_{3j} = (1-\xi_j)^3/6$, $G_{4j} = 1-\xi_j$ for the beam with S as the right end;
- $T_{33} = 2$, $T_{34} = 6$, $T_{44} = 6$, $G_{3j} = 1-\xi_j$, $G_{4j} = 1$, $S_4^n = (n\pi)^3(-1)^n$ for the beam with F as the right end.

Table 1. Comparison of the first five natural frequencies of a rectangular duct with S-S boundary conditions.

Sr. No.	Static Beam Method	Lee Paper[3] Results	Transfer Matrix Method	FEM Results
1	97.97	97.97	97.87	97.87
2	113.16	113.16	113.04	113.03
3	129.81	129.82	125.47	126.81
4	138.76	138.76	138.62	138.59
5	141.41	141.41	140.05	139.88

Table 2. Comparison of the first five natural frequencies of a rectangular duct with C-C boundary conditions.

Sr. No.	Static Beam Method	FEM Results
1	99.27	99.16
2	117.98	117.79
3	130.79	128.32
4	145.27	143.93
5	148.43	148.19

Table 3. Comparison of the first five natural frequencies of a rectangular duct with C-S boundary conditions.

Sr. No.	Static Beam Method	FEM Results
1	98.57	98.46
2	115.39	115.24
3	130.26	127.53
4	143.19	141.76
5	143.34	143.11

Table 4. Comparison of the first five natural frequencies of a rectangular duct with C-F boundary conditions.

Sr. No.	Static Beam Method	FEM Results
1	94.15	93.65
2	104.69	104.30
3	125.83	125.18
4	127.45	—
5	135.32	132.10

3. RESULTS AND DISCUSSIONS

To illustrate the validity and the accuracy of the methods, some numerical results have been presented and compared with the literature results and the FEM results. Lack of literature data for other than simply supported axial boundary conditions motivates validation with the results from the FEM analysis. Typical dimensions of duct and material properties used in the calculation are $L_1 = 0.4$ m, $L_2 = 0.3$ m, $L_3 = 1.5$ m, and the thickness $h = 0.005$ m. The material properties are: Young's modulus $E = 71$ GPa, Poisson's ratio $\nu = 0.29$, and density $\rho = 2770$ kg/m^3.

Tables 1 to 4 consist of comparisons of the natural frequency for a simple supported rectangular duct with aluminium materials. Table 1 shows the results comparison of different methods for an aluminium rectangular duct. As mentioned earlier, the Rayleigh-Ritz method with static beam functions as admissible functions is capable of incorporating other boundary conditions. These results are compared with the FEM analysis results. Tables 2, 3, and 4 show a comparison of the results for the different boundary conditions like C-C, C-S, and C-F, respectively for the aluminium rectangular duct.

FEM analysis has been carried out using commercial software (ANSYS),[9] in which shell elements are used with 30 elements per side. The Block Lanczos modal analysis scheme is used for calculating natural frequencies.

Results for the S-S axial boundary conditions are compared with the Lee paper, which also uses the Rayleigh-Ritz method but with different admissible functions.[3] The values match ex-

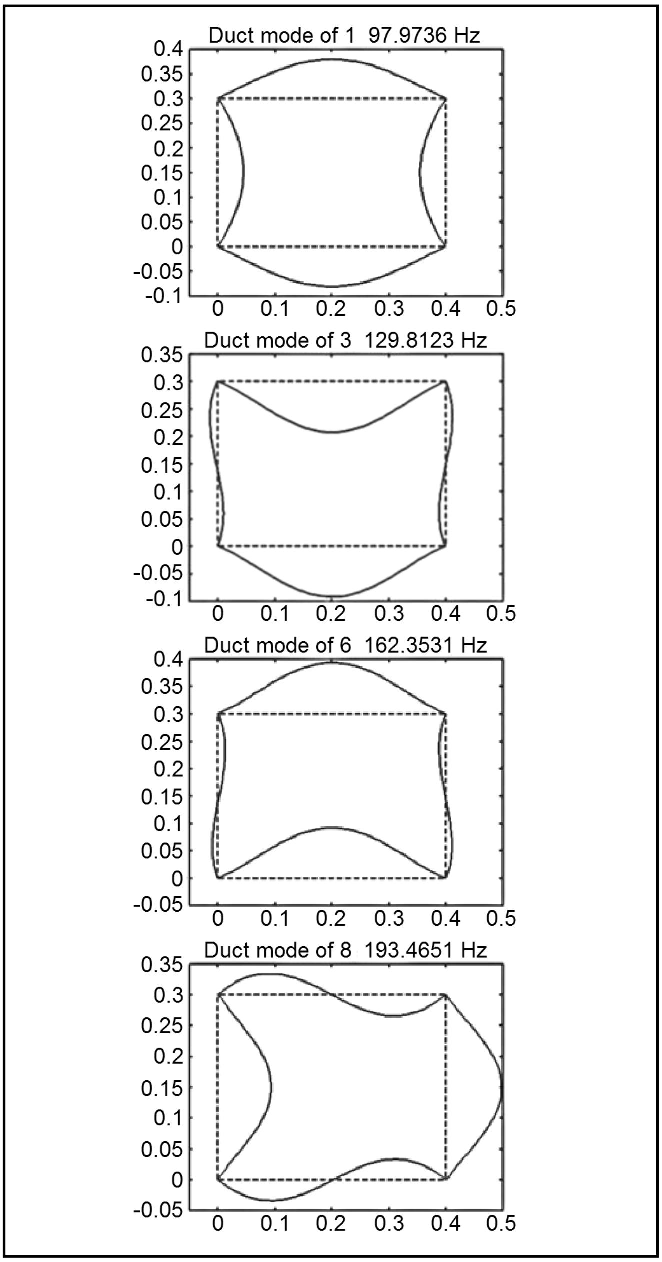

Figure 3. Mode shapes for the 1st, 3rd, 6th, and 8th natural frequencies of a rectangular duct with S-S boundary conditions.

actly with the values given by the present method (can be seen from first two columns of Table 1). The results are also compared with the transfer matrix method and the FEM results. The error observed is less than 5%. So a good amount of accuracy can be seen within these results. The same thing can be observed for the other axial boundary conditions. Results are shown in Tables 2, 3, and 4. The mode shapes are plotted and are shown in Fig. 3. Dominantly, the symmetric-symmetric (S-S) and symmetric-antisymmetric (S-AS) modes can be observed at the first few frequencies, and the antisymmetric-antisymmetric (AS-AS) modes can be observed at higher frequencies.

3.1. Engineering Data

Now this validated analytical model is used to generate values of a non-dimensional frequency parameter (λ) for different standard dimensions of the rectangular ducts. The dimensions of the ducts are divided into two ratios, one is a side ratio represented by 'S_1.' The other one is an aspect ratio represented by 'S.' The non-dimensional frequency (λ) values have been given for the different combinations of these ratios. The ratios used are 0.25, 0.5, 0.75, and 1. According to the dimension of the duct, one has to decide both of the ratios, then, from the table, select the appropriate λ value for the combination of these ratios. Eq. (13) can be used to calculate the natural frequencies in Hz from this non-dimensional value. This non-dimensional frequency parameter is independent of the material properties except for the Poisson's ratio, which is used as 0.29 to generate these values. Frequency (f) in Hz is given by

$$f = \frac{\lambda}{2\pi \times L_3^2} \sqrt{\frac{Eh^2}{12\rho\left(1-\nu^2\right)}}; \tag{13}$$

where L_3 and h are the length and thickness of the duct, respectively, and E, ρ, and ν are Young's modulus, density, and Poisson's ratio, respectively.

Tables 5 to 8 contain the values of λ for the first four natural frequencies of the rectangular duct. This data is generated for different combinations of aspect ratios and side ratios and also for different axial boundary conditions like S-S, C-C, C-S, and C-F, respectively.

Table 5. The non-dimensional frequency parameter (λ) for the S-S axial boundary condition.

Mode no.	$S_1 \downarrow \ \backslash \ S \rightarrow$	0.25	0.5	0.75	1
1	0.25	1678.81	424.56	192.37	111.19
2		1698.35	444.75	213.57	130.32
3		1731.41	480.53	227.03	133.55
4		1779.04	503.55	245.79	150.33
1	0.5	2066.62	522.62	236.72	136.69
2		2090.51	546.78	261.36	161.90
3		2130.53	588.06	295.12	168.77
4		2187.11	647.61	304.25	189.31
1	0.75	2409.82	609.41	276.02	159.34
2		2437.71	637.34	304.05	187.50
3		2484.11	684.12	351.20	211.54
4		2549.40	750.01	370.74	233.18
1	1	2536.54	641.52	290.61	167.78
2		2566.14	671.13	320.21	197.39
3		2615.41	720.48	369.56	246.74
4		2684.52	789.57	438.65	254.14

Table 6. The non-dimensional frequency parameter (λ) for the C-C axial boundary condition.

Mode no.	$S_1 \downarrow \ \backslash \ S \rightarrow$	0.25	0.5	0.75	1
1	0.25	1679.71	426.02	194.49	114.12
2		1701.64	450.18	221.69	132.86
3		1739.22	492.66	228.86	144.41
4		1790.91	504.81	252.95	160.12
1	0.5	2067.81	524.15	238.81	139.48
2		2094.34	552.26	269.08	171.01
3		2139.32	600.20	296.77	171.96
4		2200.11	657.45	320.45	197.92
1	0.75	2411.15	611.05	278.14	162.07
2		2441.91	643.01	311.65	197.15
3		2494.03	696.64	367.04	213.58
4		2563.62	769.22	372.31	240.96
1	1	2537.91	643.21	292.76	170.52
2		2570.52	676.93	327.85	206.98
3		2625.82	733.28	385.44	256.09
4		2699.31	808.97	447.52	261.29

3.2. Empirical Relation

In the above section, the non-dimensional frequency parameter (λ) has been given for different duct geometry dimensions,

Table 7. The non-dimensional frequency parameter (λ) for the C-S axial boundary condition.

Mode no.	$S_1 \downarrow \ \backslash \ S \rightarrow$	0.25	0.5	0.75	1
1	0.25	1679.23	425.22	193.32	112.46
2		1700.02	447.36	217.33	131.43
3		1735.07	486.24	227.84	138.50
4		1784.83	504.12	249.11	154.78
1	0.5	2067.24	523.31	237.67	137.93
2		2092.51	549.47	265.01	166.55
3		2134.62	593.78	295.86	169.76
4		2193.55	656.79	311.88	193.27
1	0.75	2410.47	610.15	276.98	160.56
2		2439.91	640.18	307.70	192.02
3		2488.83	690.04	358.68	212.45
4		2556.35	759.26	371.44	236.80
1	1	2537.11	642.28	291.58	169.01
2		2568.42	674.05	323.90	201.91
3		2620.36	726.50	377.07	255.02
4		2691.81	798.94	446.67	255.68

Table 8. The non-dimensional frequency parameter (λ) for the C-F axial boundary condition.

Mode no.	$S_1 \downarrow \ \backslash \ S \rightarrow$	0.25	0.5	0.75	1
1	0.25	1673.84	419.56	187.35	106.12
2		1687.01	433.38	201.87	121.26
3		1714.45	462.46	222.62	125.87
4		1777.71	499.18	232.96	139.24
1	0.5	2060.52	516.49	230.60	130.58
2		2076.94	533.24	247.76	148.15
3		2109.71	567.12	282.94	164.01
4		2152.16	616.66	290.38	177.96
1	0.75	2402.53	602.24	268.88	152.23
2		2419.63	621.66	288.55	172.15
3		2450.82	660.51	327.82	206.34
4		2506.91	719.04	365.55	211.42
1	1	2528.80	633.90	283.02	160.24
2		2549.34	654.50	303.83	181.26
3		2590.37	695.72	345.11	222.43
4		2651.32	756.99	407.09	248.42

Table 9. Values of constant 'λ_0' in an empirical Equation (14).

Axial boundary condition	Value of constant
S-S	169
C-C	171.5
C-S	170
C-F	165

from which one can calculate the first four natural frequencies directly for standard-dimension ducts. In this section, the empirical relation has been presented, which will be useful to get the non-dimensional frequency parameter (λ) for any combination of aspect ratios between 0.25 to 1 and side ratios between 0.25 to 1. This empirical relation has been formed by performing curve fitting for the above generated data. The empirical relation is of the form

$$\lambda = \lambda_0 \times S^{-1.96} \times S_1^{0.31}; \tag{14}$$

where λ_0 is constant, which depends on the axial boundary condition. Table 9 represents the values of constant 'λ_0' for different cases.

This empirical relation is useful for calculating the first fundamental frequency of a rectangular duct with different axial boundary conditions.

4. CONCLUSIONS

Free vibration analysis of rectangular ducts with different axial boundary conditions is important for understanding the vibration behaviour of these ducts in HVAC systems. A procedure is developed to calculate natural frequencies and mode shapes of a rectangular duct with different axial boundary conditions based on the Rayleigh-Ritz method. The Rayleigh-Ritz method, with a set of static beam admissible functions, has been used to consider different axial boundary conditions. This is one of the distinct advantages of using the proposed method. The results have been presented for the typical rectangular-duct dimensions. Proposed model results are validated through comparison of the known values in the literature and the results from the FEM method. Results are in agreement with accuracy more than 95%. This validated analytical model has been used to generate the engineering data, which will help engineers calculate the first four natural frequencies for different rectangular-duct dimensions. The empirical relation has been proposed based on engineering data. It will be helpful to calculate the first fundamental frequency of a rectangular duct for any combination of aspect ratios and side ratios in the range of 0.25 to 1 and also for different axial boundary conditions.

ACKNOWLEDGEMENT

The authors would like to thank the Indian Institute of Technology Hyderabad, for providing the required resources to conduct the current research work.

REFERENCES

[1] Azimi S, Soedel W., and Hamilton J.F. Natural frequencies and modes of cylindrical polynomial ducts using receptance method, *Journal of Sound and Vibration*, **109** (1), 79–88, (1986).

[2] Yamad G. and Kobayashi K. Comments on natural frequencies and modes of cylindrical polygonal ducts using receptance methods, *Journal of Sound and Vibration*, **115**, 363–364, (1987).

[3] Lee H. P., Natural frequencies and modes of cylindrical polygonal ducts, *Journal of Sound and Vibration*, **164**, 182–187, (1993).

[4] Irea T., Yamada G., and Ida H. Free vibration of longitudinally stiffened prismatic shells with and without partitions, *Journal of Sound and Vibration*, **102** (2), 229–241, (1985).

[5] Mohan S. J. and Pratap R. A natural classification of vibration modes of polygonal ducts based on group theoretical analysis, *Journal of Sound and Vibration*, **269**, 745–764, (2004).

[6] Zhou, D. Natural frequencies of rectangular plates using a set of static beam functions in Rayleigh-Ritz method, *Journal of Sound and Vibration*, **189** (1), 81–87, (1996).

[7] Zhou, D. and Cheung, Y. K. Free vibration of line supported rectangular plates using a set of static beam functions, *Journal of Sound and Vibration*, **223** (2), 231–245, (1996).

[8] Venkatesham B., Tiwari, M., and Munjal M. L., Prediction of breakout noise from a rectangular duct with compliant walls, *International Journal of Acoustics and Vibration*, **16** (4), 180–190, (2011).

[9] ANSYS 13, User Manual, ANSYS Inc.